

DESIGN CONSIDERATIONS FOR REACTION CONTROL SYSTEMS

Artem A. Dyakonov⁽¹⁾, Chris E. Glass⁽²⁾, Karl T. Edquist⁽³⁾, Mark Schoenenberger⁽⁴⁾, Pawel Chwalowski⁽⁵⁾, John Van-Norman⁽⁶⁾, William I. Scallion⁽⁷⁾, Chun Tang⁽⁸⁾, Michael J. Wright⁽⁹⁾, F. McNeil Cheatwood⁽¹⁰⁾, Brian R. Hollis⁽¹¹⁾, Victor R. Lessard⁽¹²⁾, Naru Takashima⁽¹³⁾

⁽¹⁾NASA LaRC, M/S 489, Hampton, VA, USA, 23681, artem.a.dyakonov@nasa.gov

⁽²⁾NASA LaRC, M/S 408A, Hampton, VA, USA, 23681, c.e.glass@nasa.gov

⁽³⁾NASA LaRC, M/S 489, Hampton, VA, USA, 23681, karl.t.edquist@nasa.gov

⁽⁴⁾NASA LaRC, M/S 489, Hampton, VA, USA, 23681, mark.schoenenberger-1@nasa.gov

⁽⁵⁾AMA, 303 Butler Farm Roads, Suite 104A, Hampton, VA, USA, 23666, pawel.chwalowski-1@nasa.gov

⁽⁶⁾AMA, 303 Butler Farm Roads, Suite 104A, Hampton, VA, USA, 23666, john.w.vannorman@nasa.gov

⁽⁷⁾NASA LaRC, M/S 408A, Hampton, VA, USA, 23681, w.i.scallion@larc.nasa.gov

⁽⁸⁾ELORET, NASA ARC, M/S 230-2, Moffett Field, CA, USA, 94035, ctang@mail.arc.nasa.gov

⁽⁹⁾NASA ARC, M/S 230-2, Moffett Field, CA, USA, 94035, michael.j.wright@nasa.gov

⁽¹⁰⁾NASA LaRC, M/S 489, Hampton, VA, USA, 23681, f.m.cheatwood@nasa.gov

⁽¹¹⁾NASA LaRC, M/S 408A, Hampton, VA, USA, 23681, brian.r.hollis@nasa.gov

⁽¹²⁾GENEX SYSTEMS, 1919 Commerce Drive, Suite 160, Hampton, VA, USA, 23666, victor.r.lessard@nasa.gov

⁽¹³⁾APL, 11100 Johns Hopkins Rd, Laurel, MD, USA, 20723, naruhisa.takashima@jhuapl.edu

ABSTRACT

The next generation of Mars exploration landers must precisely deliver scientific payloads to sites of interest, unlike previous Mars missions. The past missions, such as Viking and Pathfinder, performed landings to within 100s of kilometers from their targets using an unguided atmospheric entry. Guided entry of a capsule with a relatively high lift-to-drag ratio will allow landing to within 10s of kilometers from the target with a significantly more massive payload. Guided lifting entry may require the use of a reaction control system (RCS) for both attitude correction and entry guidance maneuvers. Various aspects of the entry, descent and landing (EDL) system performance may be impacted by the operation of the RCS during entry. This paper illustrates the risks that arise from the gasdynamic interaction of the entry vehicle (EV) and RCS, and which require attention in the areas of aerodynamics and control, and aerothermal environments. This paper will review the methods to address the design challenges associated with integration of RCS into the atmospheric entry system. Among these challenges is the analysis of the potential for the aerodynamic interference due to both the direct jet plume impingement and more complex plume interactions with the wake flow. These interactions can result in enhanced aeroheating, requiring that a

different approach to the thermal protection system (TPS) selection and sizing be used. The recent findings for Mars Science Laboratory and Mars Phoenix will be presented to help illustrate some of the phenomena. In addition, design solutions that mitigate interaction effects will be discussed.

NOMENCLATURE

Symbols

$a_{0,1,2,3}$	Viking base correction coefficients
$\alpha_{x,y,z}$	Angular acceleration
base	backward facing part of the capsule (in reference to capsule forces)
C_A	Axial force coefficient
C_p	Pressure coefficient
C_D	Drag coefficient
cg, CG	Center of mass location
CL	Lift coefficient
EDL	Entry descent and landing
$I_{xx,yy,zz}$	Moments of inertia
L/D	Lift to drag ratio
$M_{x,y,z}$	Axis moments
M	Mach number
M_∞	Free stream Mach number
$m/C_D A$	Ballistic coefficient
P_b	Base pressure

RCS Reaction control system
 TPS Thermal Protection System

INTRODUCTION

As a vehicle enters an atmosphere, it interacts with the surrounding gas. The interaction produces aerodynamic forces and moments that act on the vehicle during entry, and in the process, reduce the vehicle kinetic energy to an acceptable value for the deployment of a decelerator, if so equipped, or to start the powered descent as shown in Figure 1. The interactions between the vehicle and the surrounding

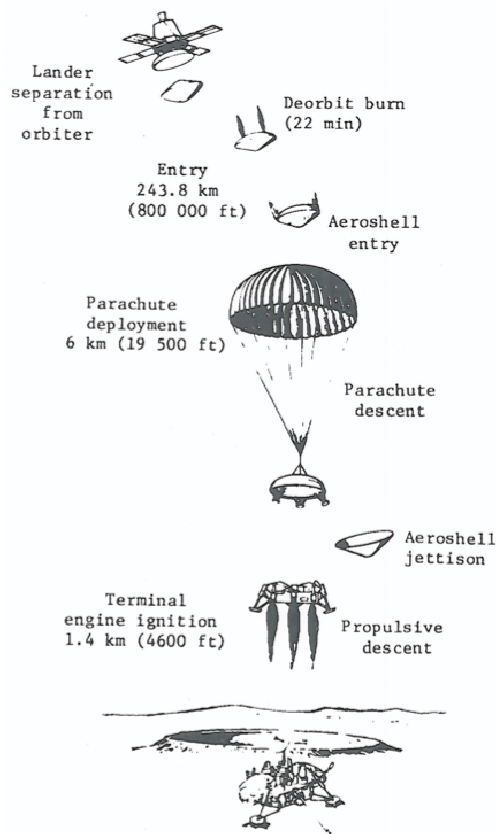


Figure 1. Example of EDL sequence (Viking)

flow, which are of importance to this paper, occur during hypersonic and supersonic flight. In these regimes, flow around the capsule is characterized by the presence of the bow shock ahead of the capsule, multiple expansion waves around the forebody shoulder, a massively separated wake flow field, and a complex recompression shock system behind the vehicle as shown in Figure 2. Depending on the

capsule shape and size and the free stream conditions, the flow around it may be laminar, transitional, or turbulent. Because of the large amount of energy that must be dissipated during entry, capsules are shaped to produce large amounts of drag with little lift, hence low lift-to-drag ratios. While drag, experienced by the vehicle during entry reduces the vehicle's total energy, lift can be used to alter its course. Lift can be obtained by flying the axisymmetrically-shaped capsule at an angle-of-attack, either by CG offset or by using a hypersonic trim tab. The Mars atmosphere is very thin¹, but enough aerodynamic lift can be generated to maneuver and extend the flight path and allow drag to bleed more energy in the denser atmosphere. Thus, a vehicle with a large ballistic coefficient ($m/C_D A$) can be landed at a the target site far above the mean ground level².

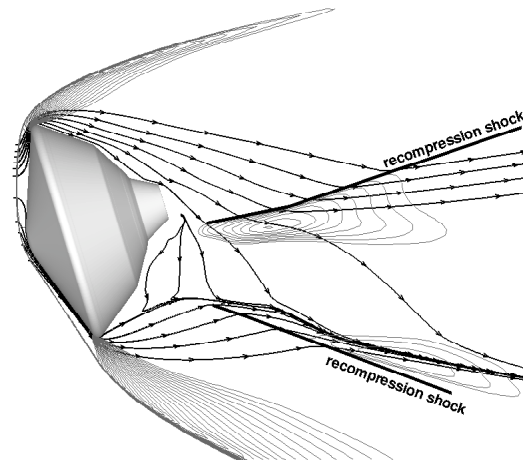


Figure 2. Flow past MSL capsule at Mach 18.1, $L/D=0.24$

The next generation of Mars entry systems will use lift for guidance³. During entry, a bank angle modulation, which controls the lift vector, is employed by means of a reaction control system to assure correct conditions are met for the parachute deployment and precision landing within 10s of kilometers from the site of interest. Also, good knowledge of the capsule aerodynamics is necessary to confidently simulate its flight in programs such as POST⁴ (POST is an acronym for Program to Optimize Simulated Trajectories). Therefore, interaction effects of the entry vehicle reaction control system on aerodynamics must be understood for the entire flight regime they are used.

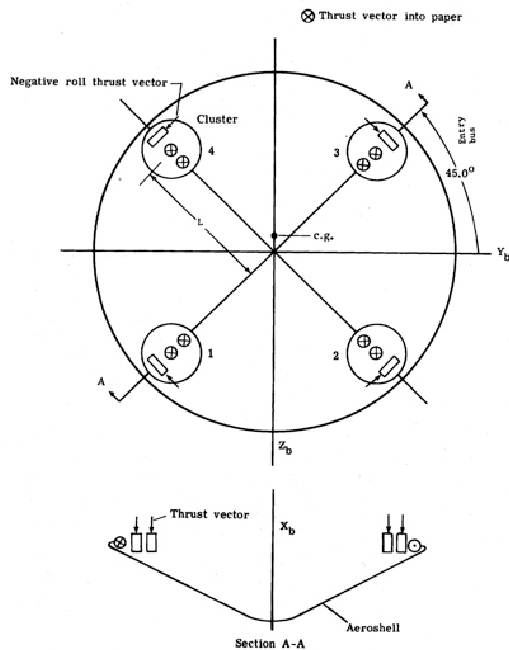


Figure 3. Viking RCS

REACTION CONTROL SYSTEM (RCS)

For precision landing, the entry vehicle must have greater control authority over its lift vector and be able to quickly respond to the atmospheric variations and static and dynamic instabilities than traditional ballistic-trajectory, spin-stabilized entry vehicles. Clearly, there is a need for a three-axis stabilized system such as an RCS to accommodate a precision landing. Also, the RCS should be able to provide angular rates sufficient for maneuvering, and be efficient in its use of fuel. This typically places requirements not only on the available axis torques but also on the moment arms when locating the RCS thrusters.

Three three-axis stabilized systems have flown to Mars: Viking 1 and 2, and MPL (Mars Polar Lander). Phoenix lander (MPX), scheduled for launch in August 2007 is comparable to MPL in design, and the names of the two will be used interchangeably because the two entry vehicles are largely equivalent. All these systems used a group of rocket engines that are fired into the wake of the

capsule, and are placed in such a way that their thrust produces the torques, necessary to control the attitude and attitude rates. Additionally, Viking probes, which flew lift-up trajectories (Table 1) used RCS to keep the lift vector pointed straight up to maximize the altitude at parachute deployment, to enable a landing at up to +3.05 km with respect to the mean surface level of Mars (see Ingoldby⁵). The Viking reaction control system, shown in Figure 3 provided independent three-axis control starting shortly after separation from the orbiter, until aeroshell jettison. Viking RCS also provided the 22-minute de-orbit burn, necessary to alter the trajectory for Mars entry. The system included 12 engines, each producing maximum 36N thrust, which were placed in clusters near the vehicle's maximum diameter⁶.

Mars Science Laboratory (MSL), currently in final design phase and scheduled to be launched in 2009 will employ active guidance to within 10 kilometers (no wind) from its target. To control the attitude and attitude rates, and the direction of the lift vector, MSL entry capsule has a reaction control system, composed of 8 engines capable of ~ 267N thrust each. The available control torques and inertial properties of Viking, MPL and MSL are shown in Table 2 for comparison. Although still being designed, the present MSL reaction control system configuration, shown in the Figure 4, is evaluated. In addition, results from two other configurations are presented subsequently for comparison.

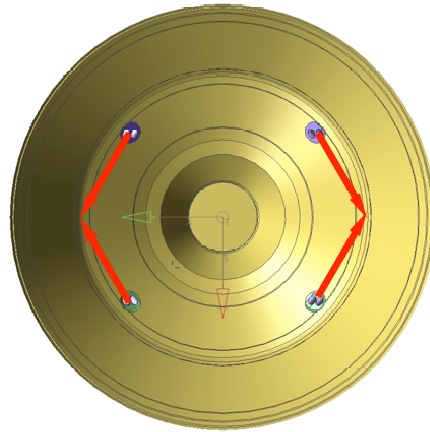


Figure 4. Candidate MSL RCS Layout. Red arrows represent jet directions.

RCS should be able to provide angular rates sufficient for maneuvering, and be efficient in its use of fuel. This typically places requirements not only on the available axis torques, but also on the moment arms.

CAPSULE WAKE INTERACTION WITH THE RCS JET

The complex structure of the base flow, which is illustrated in the Figure 2, is analyzed by a range of CFD methods. Structured and unstructured grids, perfect and real gas chemistry, thermal and chemical equilibrium and non-equilibrium, laminar and turbulent, and steady and time-accurate solutions are used to predict the environments in the wake of the

entry vehicle. Typical wake flow is unsteady, with multiple time constants because of the complex vortical structures. Three dimensional shear layers, mixed character of the flow, rapid expansions and possible turbulence complicate the reliable prediction of the wake behavior. Extensive use of the ground-based testing is employed to validate the predictive capability of CFD.

Until recently, the accurate solution of wake environments wasn't critical because without RCS interactions contribution of the aftbody aerodynamics and aerothermodynamics was small compared to that of the forebody. The need to analyse RCS efficacy prompted reevaluation of the computational and experimental tools. The interaction phenomena that are produced by the jet

Table 1. Comparison of Mars Entry Capsules




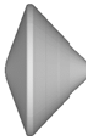
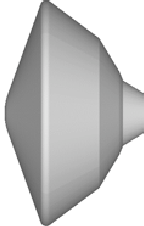
	Viking 1/2	Pathfinder	MER A/B	Phoenix	MSL
					
Diameter, m	3.5	2.65	2.65	2.65	4.5
Entry Mass, kg	930	585	840	602	2919
Landed Mass, kg	603	360	539	364	1541
Landing Altitude, km	-3.5	-1.5	-1.3	-3.5	+1.0
Landing Ellipse, km	420 x 200	100 x 50	80 x 20	75 x 20	< 10 x 10
Relative Entry Vel., km/s	4.5/4.42	7.6	5.5	5.9	> 5.5
Relative Entry FPA, deg	-17.6	-13.8	-11.5	-13	-15.2
m/(C_DA), kg/m²	63.7	62.3	89.8	65	126
Turbulent at Peak Heating?	No	No	No	No	Yes
Peak Heat Flux, W/cm²	24	115	54	56	243
Hypersonic α, deg	-11.2	0	0	0	-15.5
Hypersonic L/D	0.18	0	0	0	0.24
Control	3-axis	Spinning	Spinning	3-axis	3-axis
Guidance	No	No	No	No	Yes

Table 2. Comparisson of RCS Authority and Capsule Moments of Inertia

	N-m			Kg-m ⁴			deg/sec ²		
	M _x	M _y	M _z	I _{xx}	I _{yy}	I _{zz}	α_x	α_y	α_z
Viking 1,2	152.7	146/-159.4	108	536	423	786	16.3	19.8/-21.6	7.9
MPL/Phoenix	10.7	58.07	10.06	192	189	286	3.2	17.6	2.0
MSL	675.4	980.7/-1160	705	3055	3952	4836	12.7	14.2/-16.8	8.4

and which may produce change to the aftbody aerodynamics and the aftbody aeroheating, which must be understood to certify RCS for flight. Because the jet is exhausting into the wake of the capsule, its effect is primarily concentrated on the aftbody.

Depending on the size of the jet, its location and pointing, the interaction may result in significant changes to the flowfield.

RCS AERODYNAMIC EFFECTS

Hypersonic and supersonic aerodynamics of blunt entry capsules are dominated by forces and moments that develop on the forebody heatshield. At hypersonic speeds the pressure on the aftbody is so small in comparison to the forebody pressure, that the contribution of aftbody forces and moments to the capsule aerodynamics is justifiably ignored. At supersonic speeds the aftbody pressures are not negligible in relation to forebody pressures, and must be accounted for. This is typically accomplished by applying the base pressure correction, derived from the Viking flight data⁷

$$C_{A(base)} = C_{p,b} = a_0 + \frac{a_1}{M_\infty} + \frac{a_2}{M_\infty^2} + \frac{a_3}{M_\infty^3} \quad (1)$$

where

$$\begin{aligned} a_0 &= 8.325E-03 \\ a_1 &= 1.129E-01 \\ a_2 &= -1.801E+00 \\ a_3 &= 1.289E+00 \end{aligned}$$

Variation of $C_{A(base)}$ with the Mach number is shown in the Figure 5. At supersonic speeds the aftbody contribution increases the axial force on the capsule, contributing to drag, while at hypersonic speeds the aftbody contribution has an opposite sign, indicating reduced drag. Because of the small magnitude, the contribution of the aftbody at hypersonic speeds (above Mach 8) is typically not included in the simulation. For comparison, the hypersonic axial force coefficient on the 70-degree blunt cone is typically between 1.5 and 1.7 depending on the angle-of-attack. The relationship between the aftbody force coefficient and the Mach number suggests that aftbody forces at hypersonic speeds can be neglected in comparison to the forebody forces. This approach is adequate for static aerodynamics.

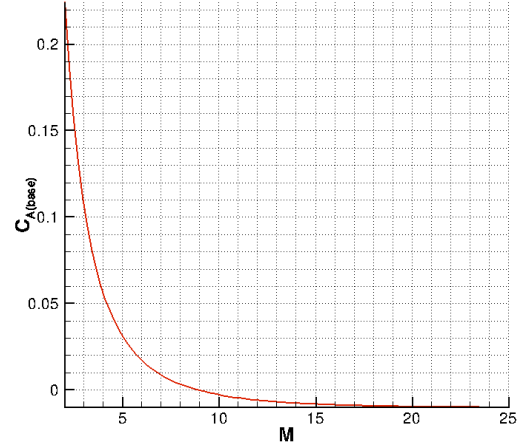


Figure 5. Base correction

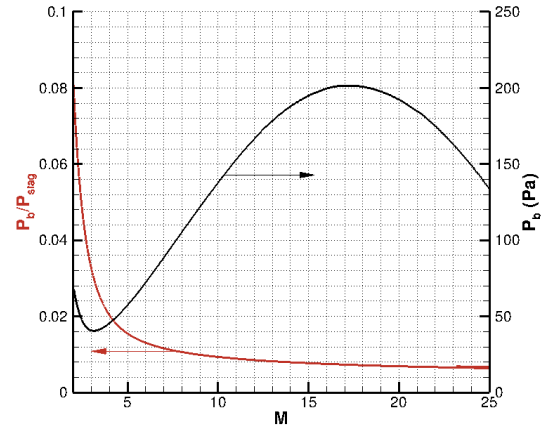


Figure 6. Base pressure and its ratio to the stagnation pressure, MSL 06-05 trajectory

When an RCS jet is fired, the aftbody will experience a sudden change in the pressure distribution because of the interaction between the wake and the jet plume. This change in the surface pressures translates into the change of the capsule moments, which may be significant as compared to the ideal RCS torque. Because the flow direction and pressure in the wake determines the magnitude of the interaction between the jet plume and the wake, it is necessary to consider the pressure variation in the wake of the capsule as a function of free stream conditions. Figure 6 shows the pressure in the wake P_b and the ratio of P_b to stagnation pressure for MSL entry trajectory. Peak aftbody pressure occurs at a hypersonic Mach number. This has a scaling effect on the aerodynamic moments, induced by RCS interaction.

For example, consider a case of yaw correction for one of the proposed MSL RCS, evaluated at Mach 18.1. Figure 7 illustrates the intersecting plume geometry and the effect of plumes on the surface pressures for this case. The mean yawing moment about CG, produced by the aftshell due to the induced pressure asymmetry is computed from CFD to be around 500 N-m. Ideal yawing RCS authority for this case is -561 N-m. These numbers indicate a predicted negation of almost all control authority in yaw at Mach 18. The largest contribution to the adverse torque is produced by the pressure increase at the near-shoulder region, where an increase in pressure over a broad region is predicted. The X-moment arm is a maximum near the shoulder, as shown in the Figure 8. Similar analysis at Mach 2.5 predicts an opposing torque on the order of 1/3 of the ideal authority. Later iterations of the RCS layout were found to produce smaller disturbances in the wake flowfield, resulting in acceptable overall performance. Analyses such as these are important to screen configurations that do not perform as ideally predicted.

The illustrated example is one of CFD solutions in the ongoing effort to quantify, computationally and experimentally, the extent of the interaction between the RCS and aerodynamics for planetary entry vehicles. This case is one of the most alarming cases yet, and it showed that significant interactions may be produced at the flight regimes in which the aftbody aerodynamics are a small contributor to the total capsule aerodynamics, and for that reason, are hard to quantify.

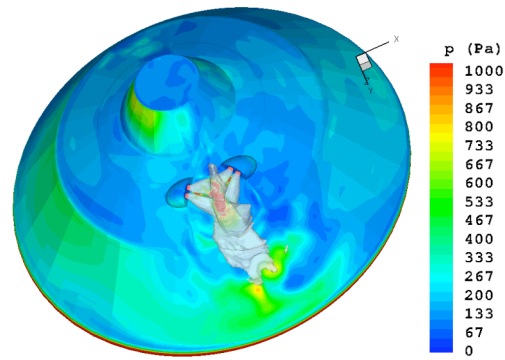


Figure 7. Candidate MSL RCS, surface pressures, Mach 18.1

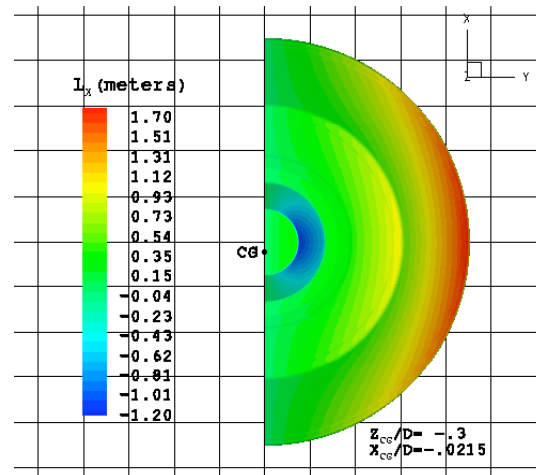


Figure 8. X-moment arm lengths for each point on the backshell w.r.t. CG

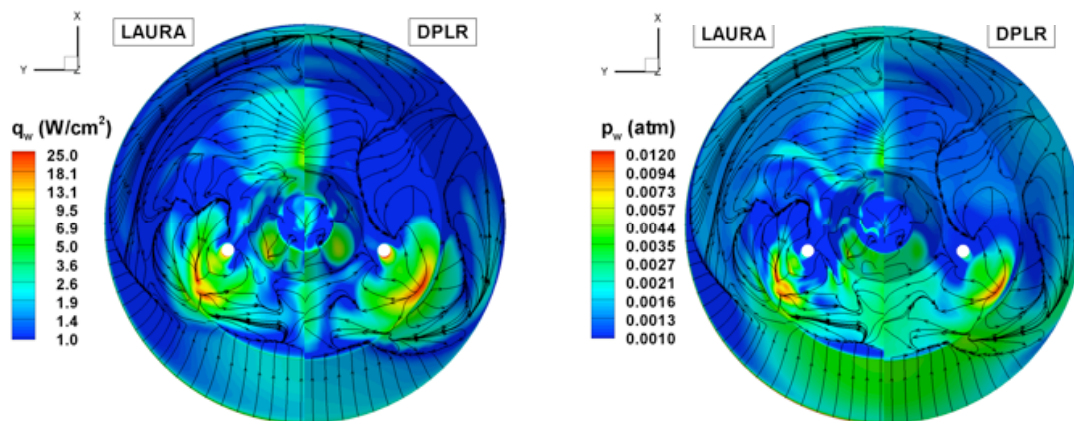


Figure 9. Computed heating rate and surface pressure comparisons, LAURA/DPLR, laminar, unmargined

RCS AEROTHERMAL EFFECTS

A number of discussions of the aerothermal environments for Mars entry vehicles have been presented^{8,9,10}. Aeroheating codes are used extensively to compute entry environments with the supporting experimental programs that allow the numerical methods to be grounded in test data¹¹. Most of this work is focused on the forebody and attached flow regions of the aftbody. Because of the relatively benign environments in the recirculating regions of the wake, appropriate uncertainties¹⁰ are applied to define TPS operational environment. Significant change to the aerothermal environments may occur due to the RCS jet interference. The RCS thruster, aimed into the oncoming flow forms a horseshoe-shaped pressure front, resulting in significant heating augmentation when compared with the non-RCS case. To gain confidence in these predictions, code comparisons are performed. Figure 9 shows the comparison of surface heating and surface pressure, computed with LAURA and DPLR for the same system, and using a similar modeling approach. Although the results presented in the figure qualitatively compare well, other challenges concerning RCS interactions must be addressed. Some of the outstanding challenges that remain in modeling of RCS are: free jet boundaries, chemical interactions between the effluent and wake, and chemical effects of the effluent on the TPS. Also, TPS jets are typically pulsed; therefore, it is necessary to understand the response of the wake to the thruster cycle. None of the codes presently used in this RCS analysis can provide the necessary time accuracy. Calculations presented herein were performed with a constant mass flow through the jet and provide an upper bound of the RCS interaction phenomena.

RCS DESIGN PHILOSOPHY

Because of the high drag requirement, the entry capsules typically have high ratio of projected area to volume. This results in a broad subsonic shocklayer that is joined to the massively separated wake by rapidly expanding supersonic shoulder flow as shown in the Figure 2. Because the RCS engines exhaust into the wake, their jets predominantly influence the wake and not the forebody flow. The

influence of the jets on the aftbody surface pressures depends on the local and RCS flow and the jet size, placement and orientation. Because the aft-cover is primarily shaped to accommodate the payload, structure, cruise stage mounting etc. its role as an aerodynamic surface is frequently viewed as secondary. This can result in the aftshell of the shape, such that there are regions with large moment arms about the CG as shown in the figure 10. The effect that the changes in pressure distribution due to the RCS activity may have on the capsule moments is difficult to anticipate due to both the complexity of the interaction and the complexity of the surface, over which it takes place.

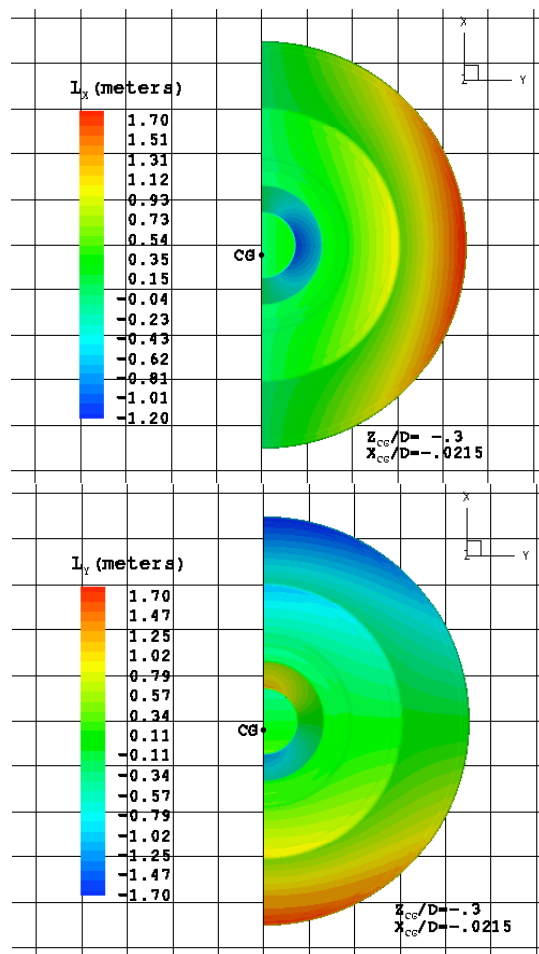


Figure 10. X-, Y-moment arm lengths for each point on the MSL backshell w.r.t. the CG

Experience with the analysis of the aerodynamic and aerothermal RCS effects has yielded several working paradigms that are being applied to the MSL RCS design. Because the interactions are strongest when the jet is aimed against the oncoming supersonic flow, it is preferred to direct RCS engines with the oncoming flow, or to place them in such a way, that the jet plumes would be contained entirely within the re-circulating region. The latter may not be possible, as the re-circulating region's shape and size may not be adequate. If strong interactions between the jet and surrounding flow are unavoidable, it may be possible to have such interactions that result in favorable capsule moments, or almost no moments. Mapping the surface moment arms can help understand where the

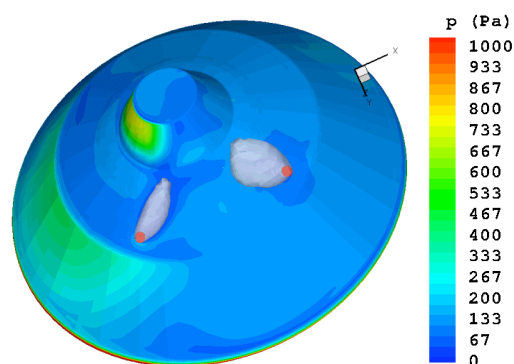


Figure 11. Current MSL RCS, Mach 18.1, yaw jets, surface pressure.

interactions can be favorable. Figure 11 illustrates the recent MSL RCS design that follows this philosophy with good success. When compared to the one, shown in the Figure 7, the reduced effects of the jets on the surface pressures are evident. Generally, achieving the same ideal control torque by a smaller engine with a larger moment arm should reduce the interactions, and should be pursued if possible.

SUMMARY

Design concerns and considerations for Mars entry vehicle RCS are presented. Vehicle precision landing requires RCS, and RCS interactions on the entry vehicle aerodynamics can be significant. Numerical methods to assess these effects are being developed and tested. Accurate characterization of RCS interference aerodynamics through experiments is challenging because the regime of

interest is hypersonic flight. Unexpected reduction or increase of thruster efficacy can interfere with flight software, reducing the performance of the EDL system. In the course of the analyses of the RCS effects several off-designs were explored to gain understanding of the design space. Based on this understanding, paradigms for RCS design were formed. These paradigms are consistent with the layout philosophy of the control system of the Viking landers. It is shown through CFD analysis that the RCS aerodynamic interaction effects depend greatly on the jet location and direction. Experiments are needed to anchor the CFD employed for the flight condition cases. In this regard, the need for instrumented flights is especially evident. Unlike the RCS interaction aerodynamic effects that can render the control system layout unusable, the aerothermal augmentation, can typically be addressed with TPS design change for the same RCS layout. In addition, CFD has been shown to be essential in mapping out the aerodynamic and aerothermodynamic design space for RCS interactions on Mars entry vehicles.

References:

1. Justus, C.G., "Mars Global Reference Atmospheric Model for Mission Planning and Analysis," *Journal of Spacecraft and Rockets*, Vol. 28, No.2, pp. 216-221, April-June 1991.
2. Dwyer-Cianciolo, A.M., Powel, R.W., Lockwood, M.K., Graves, C.A., Carman, G.L. "Effect of Entry Velocity on Landing Altitude for Ballistic and Lifting Vehicles," presentation material, November 25, 2002
3. Lockwood M. K., Powell R. W., Graves C. A., Carman G. L. "Entry System Design Considerations for Mars Landers," AAS conference paper, January 2001, Breckenridge, Colorado
4. Bauer, G.L., Cornick, D.E., and Stevenson, R. "Capabilities and Applications of the Program to Optimize Simulated Trajectories (POST)," NASA CR-2770, February 1977.
5. Ingoldby R. N. "Guidance and Control System Design of the Viking Planetary Lander," *Journal of Guidance and Control*, Vol. 1, NO. 3, MAY-JUNE 1978
6. Holmberg N. A., Faust R. P., Holt H. M. "Viking '75 Spacecraft Design and Test

- Summary; Volume 1 – Lander Design,” NASA Reference Publication 1027, 1980
7. Schoenenberger, M., Cheatwood, F.M., Desai, P.N. “Mars Exploration Rover Aerodynamic Database,” NASA LaRC, October 2003
 8. Gnoffo P. A., Weilmuenster K. J., Hamilton H. H., Olynick D. R., Venkatapathy E. “Computational Aerothermodynamic Design Issues for Hypersonic Vehicles,” Journal of Spacecraft and Rockets, Vol. 36, No. 1, January-February 1999
 9. Gnoffo P. A. “Planetary-Entry Gas Dynamics,” Annu. Rev. Fluid Mech. 1999. 31: 459-94
 10. Edquist, K.T., Dyakonov, A.A., Wright, M.J., Tang, C.Y. “Aerothermodynamic Environments Definition for the Mars Science Laboratory Entry Capsule,” AIAA 2007-1206, Reno, January 2007
 11. Hollis, B.R., Liechty, D.S., Wright, M.J., Holden, M.S., Wadhams, T.P., McLean, M., Dyakonov, A.A. “Transition Onset and Turbulent Heating Measurements for the Mars Science Laboratory Entry Vehicle,” AIAA 2005-1437, Reno, January 2005